10

Fabrication of Photonic Crystal Cavities for Terahertz Wave Resonations

Soshu Kirihara
Osaka University,
Japan

1. Introduction

Photonic crystals with periodic arrangement of dielectric media can exhibit forbidden gaps in electromagnetic wave bands through Bragg diffraction (Ohtaka; 1979, Yablonovitch; 1987, John; 1987, Temelkuran; 2000). The prohibited frequency ranges are especially called photonic band gaps. If the periodicity is changed locally by introducing a defect, localized modes appear in the band gap (Ho; 1990, Soukoulis; 1999, Noda; 1999, Kirihara; 2002a, Kanehira; 2005). Such localization function of electromagnetic waves can be applied to various devices, for example resonators, waveguides, and antennas. Three dimensional photonic crystals with a diamond structure are regarded as the ideal photonic crystal since they can prohibit the propagation of electromagnetic waves for any directions in the band gap (Ho; 1990, Kirihara; 2002b). However, due to the complex structure, they are difficult to fabricate. In our previous investigations, we have succeeded in fabricating micrometer order diamond structures by using stereolithography method of a computer aided design and manufacturing (CAD/CAM) processes (Chen; 2007a, 2007b, 2007c, 2008, Kanaoka; 2008, Miyamoto; 2008). Subsequently, structural modifications of the diamond lattice structures to control the terahertz wave propagations were investigated by using the CAD/CAM process practically (Takano; 2005, Kirihara; 2009, 2008a, 2008b). In near future industries, electromagnetic waves in a terahertz frequency range with micrometer order wavelength will be expected to apply for various types of novel sensors which can detect gun powders, drugs, bacteria in foods, micro cracks in electric devices, cancer cells in human skin and other physical, chemical and living events (Kirihara; 2009b, Exter; 1989, Clery; 2002, Kawase; 2003, Woodward; 2003, Wallace; 2004, Oyama; 2008). In this chapter, the novel stereolithography process to fabricate the micro diamond photonic crystals by using the ceramic slurry with the nanoparticles will be introduced. And, the resonation and localization properties of the terahertz waves into various types of the structural defects introduced according to theoretical electromagnetic simulations will be demonstrated.

2. Photonic crystals

2.1 Band gap formation

Photonic crystals composed of dielectric lattices form band gaps for electromagnetic waves. These artificial crystals can totally reflect light or microwave at a wavelength comparable to

the lattice spacings by Bragg deflection as shown in Fig. 1. Two different standing waves oscillating in the air and dielectric matrix form higher and lower frequency bands in the first and second Brillouin zones, respectively. The band gap width can be controlled by varying structure, filling ratio, and dielectric constant of the lattice. Structural modifications by introducing defects or varying the lattice spacing can control the propagation of light or microwaves. The band diagram of the photonic crystal along symmetry lines in the Brillouin zone is drawn theoretically. The Maxwell's equations (1) and (2) can be solved by means of plane wave propagation (PWE) method (Haus; 1994), where ω and c denote frequency and light velocity, respectively. Electronic and magnetic field Eω (r) and Hω(r) are described with the following plane wave equations (3) and (4), respectively. The periodic arrangement of dielectric constant ε(r) can be obtained as equation (5) from the crystal structure. G and k are reciprocal vector and wave vector, respectively.

$$\left[\nabla\times\left(\frac{1}{\varepsilon(\mathrm{r})}\right)\nabla\times\right]\mathbf{H}_{\omega}(\mathrm{r})=\left(\frac{\omega}{\mathrm{c}}\right)^{2}\mathbf{H}_{\omega}(\mathrm{r}) \tag{1}$$

$$\left[\frac{1}{\varepsilon(\mathrm{r})}\nabla\times\nabla\times\right]\mathbf{E}_{\omega}(\mathrm{r})=\left(\frac{\omega}{\mathrm{c}}\right)^{2}\mathbf{E}_{\omega}(\mathrm{r}) \tag{2}$$

$$\mathbf{H}_{\mathrm{k,n}}(\mathrm{r})=\sum_{\mathbf{G}}\mathbf{H}_{\mathrm{k,n}}(\mathbf{G})e^{i(\mathrm{k+G})\cdot\mathrm{r}} \tag{3}$$

$$\mathbf{E}_{\mathrm{k,n}}(\mathrm{r})=\sum_{\mathbf{G}}\mathbf{E}_{\mathrm{k,n}}(\mathbf{G})e^{i(\mathrm{k+G})\cdot\mathrm{r}} \tag{4}$$

$$\frac{1}{\varepsilon(\mathrm{r})}=\sum_{\mathbf{G}}\frac{1}{\varepsilon(\mathbf{G})}e^{i\mathrm{G}\cdot\mathrm{r}} \tag{5}$$

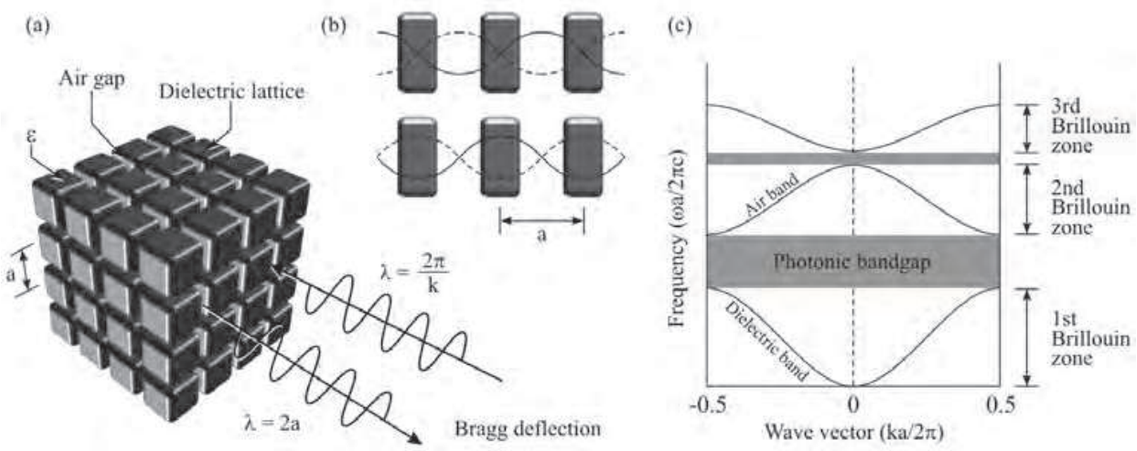

Fig. 1. Principles of photnic band gap formations in periodic arrangements of dielectric materials. Two different standing waves with higher and lower frequencies are formed in a photonic crystal, and a forbidden gap is formed between these frequencies.

2.2 Artificial crystal geometries

Typical photonic crystal structures were shown in Fig. 2. A woodpile structure (a) with simple structure of stacked rods can form the perfect photonic band gap. Photonic crystals composed of GaAs or InP were fabricated by using semiconductor process techniques (Noda; 2000). A light wave circuit (b) in the periodic structure of arranged AlGaAs pins is processed by using electron beam lithography and etching techniques (Baba; 2001). A layered structure (c) composed of Si and SiO_2 with the different dielectric constants realize light wave polarization and super prism effects (Kosaka; 1999). These layers are stacked by using self-organized growing in alternate spattering and etching. An inverse opal structure (d) is composed of air spheres with FCC structure in TiO_2, Si, Ge or CdS matrix (Cregan; 1999). At first, polystyrene spheres are arranged by using self-organization in colloidal solutions. Then, the slurry of these dielectric media is infiltrated into the periodic structure and sintered. The optical fiber (e) with photonic crystal structure can guide light efficiently along the central core (Vos; 1996). Silica fibers and glass capillaries were bundled by wire drawing at high temperature. Diamond type photonic crystals (f) composed of TiO_2, SiO_2 or Al_2O_3 can be fabricated by using stereolithography and successive sintering process. The wider perfect band gap is obtained in microwave and terahertz wave frequency ranges.

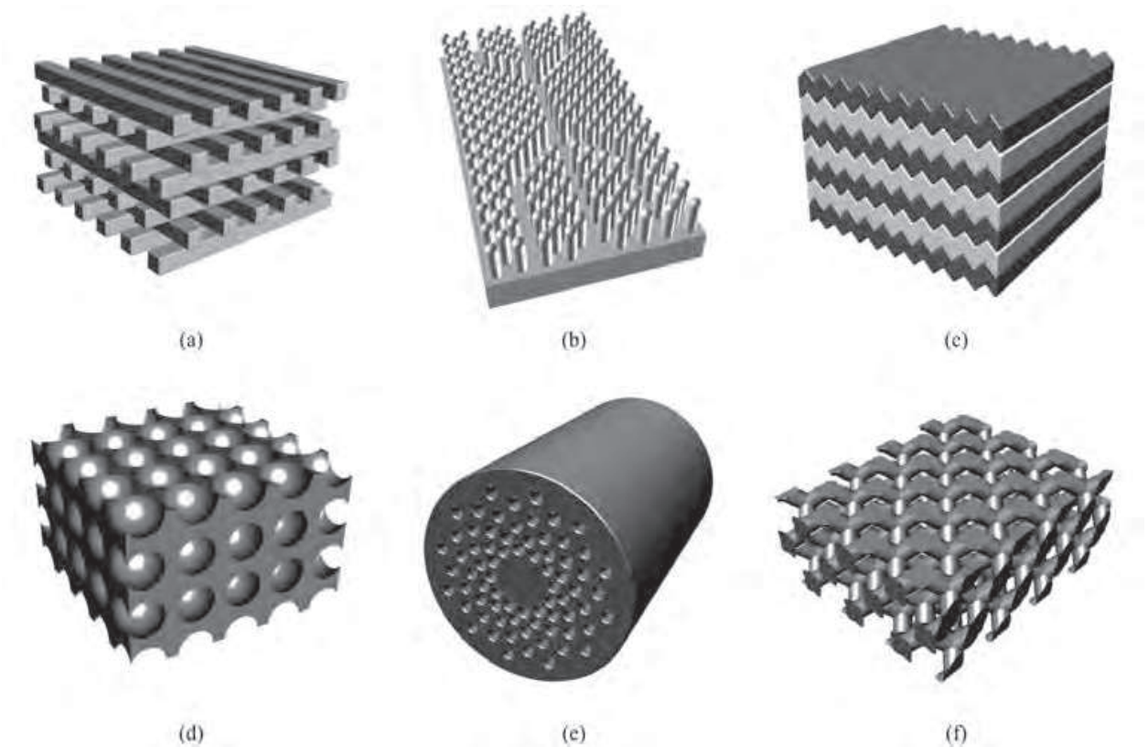

Fig. 2. Typical periodic structures of the photonic crystals with woodpile structure (a), patterned substrate (b), stacked layer (c), inverse opal structure (d), bundled fiber (e), and diamond structure (f).

2.3 Utility applications

Figure 3 shows expected applications of photonic crystal for light and electromagnetic wave control in various wavelength ranges (Kawakami; 2002). Air guides formed in a photonic

crystal with nanometer order size will be used as the light wave circuit in the perfect reflective structure. When a light emitting diode is placed in an air cavity formed in a photonic crystal, an efficient laser emission can be enhanced due to the high coherent resonance in the micro cavity. While, millimeter order periodic structures can control microwaves effectively. Directional antennas and filters composed of photonic crystals can be applied to millimeter wave radar devices for intelligent traffic system (ITS) and wireless communication system. The perfect reflection of millimeter wave by photonic crystal will be useful for barriers to prevent wave interference. Terahertz waves with micrometer order wavelength are expected to apply for various types of sensors to detect gun powders, drugs, bacteria in foods, micro cracks in electric devices, cancer cells in human skin and other physical, chemical and living events. The micrometer order photonic crystals can be applied for the terahertz wave cavities, filters and antennas.

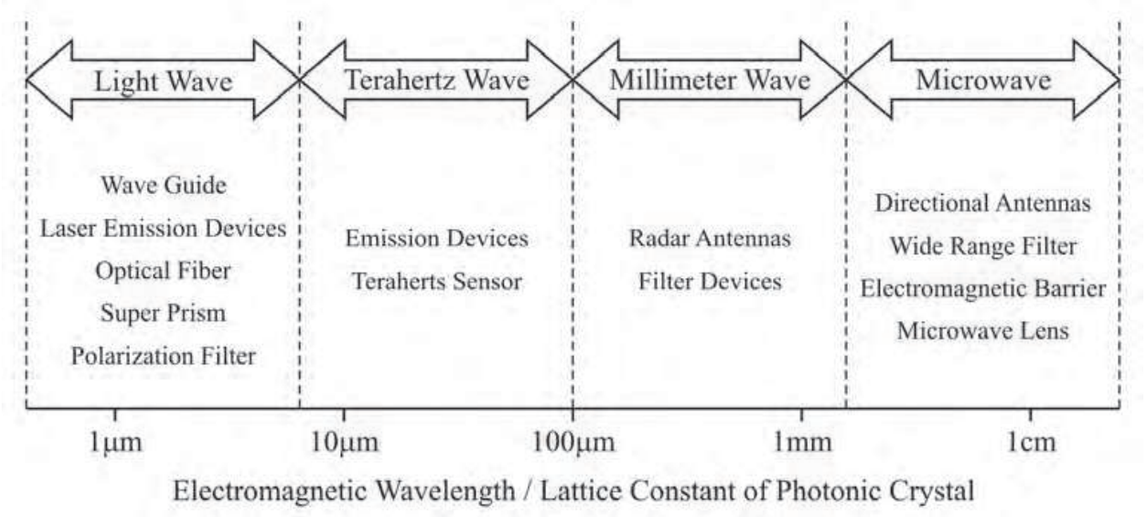

Fig. 3. Expected applications of the photonic crystal in various electromagnetic wavelengths.

3. Terahertz wave

3.1 Novel usefulness

The terahertz waves have received extensive attentions and investigations since they have a lot of interesting and applicable features in various fields such as materials, communication, medicine, and biology (Yamaguchi; 2005, Fischer; 2002, Oyama; 2009, Wallace; 2004, Hineno; 1974). It is possible to detect high explosives and ceramic blades hidden in bags, clothes, and envelopes by using terahertz waves since they can penetrate plastic, paper, and clothes without radiation damage to living bodies. It is also possible to identify toxic drugs because they have spectral fingerprints or absorption spectra. Moreover, they can distinguish cancerous areas from healthy areas due to the different absorption rates. In recent years, the terahertz waves have attracted considerable attentions as novel analytical light sources. Because the electromagnetic wave frequencies from 0.1 to 10 THz can be synchronized with collective vibration modes of saccharide or protein molecules, the terahertz wave spectroscopy are expected to be applied to various types of sensors for detecting harmful substances in human bloods, cancer cells in the skins and micro bacteria in vegetables. Moreover, the terahertz sensing technologies for aqueous phase environments in nature

fields to detecting dissolved matters directly are extremely interesting topics. However, the terahertz waves are difficult to transmit into the water solvents with millimeter order thickness corresponding to the several wavelengths due to electromagnetic absorptions (Kutteruf; 2003).

3.2 Effective control

In the previous investigations of other research groups, Fabry-perot cavities have been applied for terahertz wave resonators. However, it is theoretically unfeasible to achieve the effective single mode operation in the micro Fabry-perot resonators since electromagnetic losses of the increasing in inverse proportion to the cavity size (Akahane; 2003). Compare with this, photonic crystals can realize the single mode resonation without the electromagnetic losses through the appropriate structural design. Especially, the three dimensional diamond lattices are regarded as the ideal photonic crystal structures. Figure 4-(a) and (b) show a unit cell of the diamond photonic crystal and a electromagnetic band diagram calculated by using plane wave expansion method simulator (RSOFT Design Group Co. Ltd., USA, BandSOLVE), respectively. The artificial crystal can totally reflect the terahertz wave with the corresponding wavelength to the lattice spacing through the Bragg diffraction. The complete photonic band gap is formed to prohibit electromagnetic wave expansions for all crystal directions. In the recent investigations, the diamond structures introduced a point or plane defect were formed successfully, and localized modes with several wavelengths were observed in the cavity regions. From these obtained results, the diamond photonic crystals can be applied to low loss terahertz wave resonator.

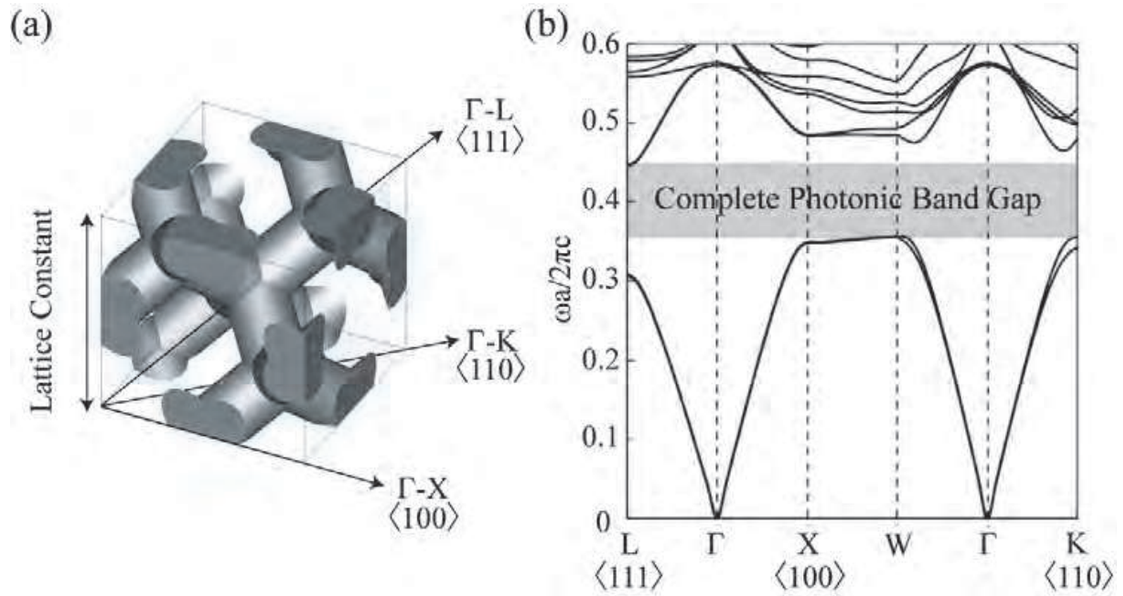

Fig. 4. A graphic image of a unit cell of the diamond structure (a), and a photonic band diagram of diamond lattice structure calculated by plane wave expansion (PWE) method (b).

3.3 Device concepts

In our investigation group, we designed and fabricated the terahertz wave resonators composed of the defects introduced photonic crystals. The micrometer order alumina

lattices with the diamond structures can resonate and localized the terahertz waves strongly into the water solvents in order to realize the higher analytical precisions. In the photonic crystal resonator, a micro glass cell including the water solvent was put between two diamond lattice structures as a plane defect. The micro structures of the dielectric lattice and resonation cavity were modelled theoretically. Subsequently, the real resonator module was fabricated successfully by using the micro stereolithographic procedure. The incident terahertz wave was reflected multiply to achieve longer optical distance in the liquid region and localized to amplify the sensing signal in the transmission spectrum. The terahertz wave properties of the resonation profiles in the transmission spectra and the localized modes in the plane defects through fabricated resonators were observed and visualized successfully by using a time domain spectroscopy and a finite difference time domain simulator, respectively.

4. Geometric design

4.1 Diffraction lattices

The electromagnetic band properties of the diamond photonic crystals were calculated theoretically to determine the geometric parameters by using the plane wave expansion method [16]. Figure 5 shows the variations of complete band gap widths as the function of aspect ratio in the dielectric lattice. In the calculation, the alumina ceramics of 9.8 in dielectric constant was assumed as the lattice material. The aspect ratio was optimized as 1.5 to create the wider band gap. Subsequently, the gap frequency can be shifted for the lower range according in inverse proportion to the lattice spacing as shown in Fig. 6. To open the band gapes in the terahertz frequencies, micro scale structural periods need to be created. The lattice constant was designed as 375 μm corresponding to the band gap frequencies from 0.3 to 0.6 THz.

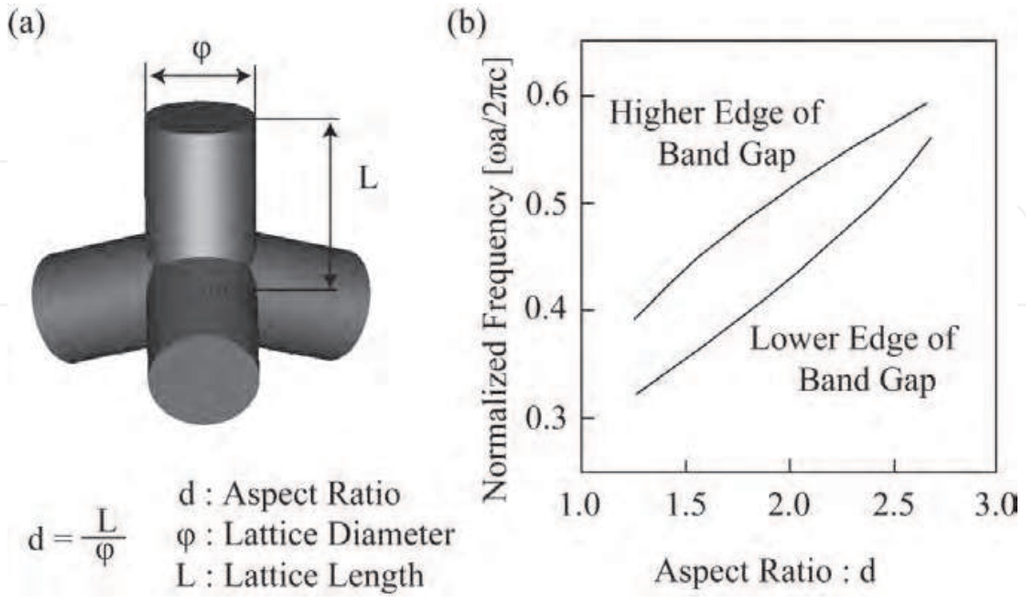

Fig. 5. Definition of aspect ratio of diamond structure (a), and the band gap width as a function of aspect of aspect ratio (b).

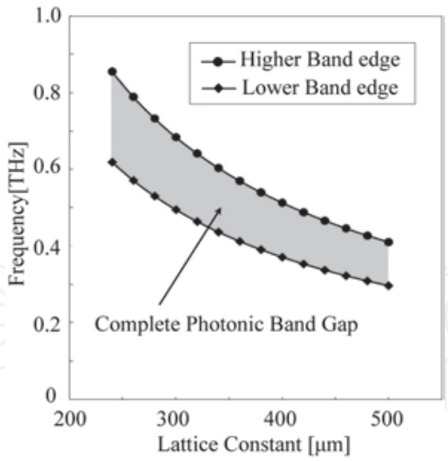

Fig. 6. Variations of electromagnetic bands as functions of lattice constants in the photonic crystals with the diamond structures.

4.2 Resonation cavity

Resonance efficiencies of the terahertz wave resonator with the diamond lattices were optimized by using transmission line modelling simulator (Flomerics Co. Ltd., UK, Micro-Stripes Ver. 7.5) of a finite difference time domain method. Figure 7 shows a computer graphic model of the terahertz wave resonator. The micro glass cell including the water was sandwiched as the plane defect between two alumina photonic crystals with the diamond lattice. The defect thickness of the resonator and the period numbers of the diamond units were selected as the principle parameters to control the resonance characteristics. The defect thickness enables to tune the resonance frequencies in the band gap as shown in Fig. 8. The plane defect was designed as the water cell of 470 μm in thickness composed of two quartz plates of 160 μm and an aqueous cavity of 150 μm. The period numbers of the diamond lattices enables to adjust the resonance qualities as shown in Fig. 9 The resonance qualities can be enhanced by increasing the period numbers, however, the localized mode of the transmission peak becomes lower through the perfect confinement of the electromagnetic wave in the defect domain. The diamond lattices composed of two units in period number were optimized and designed in order to detect the sharp localized mode peak in the transmission spectrum.

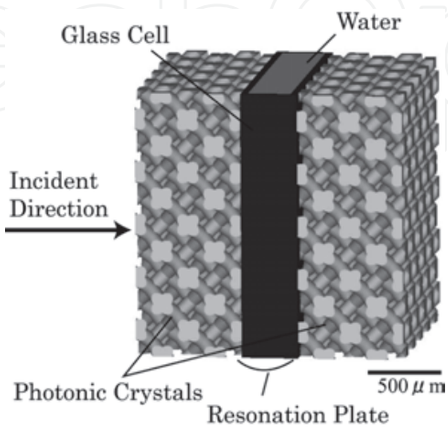

Fig. 7. A computer graphic model of a terahertz wave micro reactor.

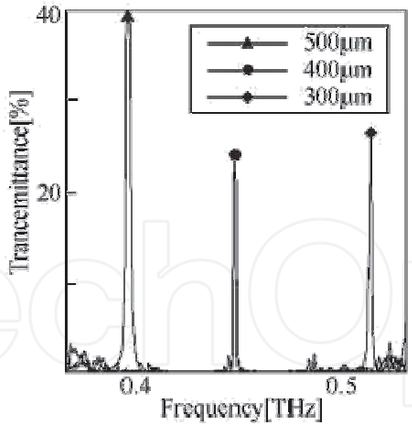

Fig. 8. Calculated localized mode formations through electromagnetic waves resonations in micro cells with various thicknesses.

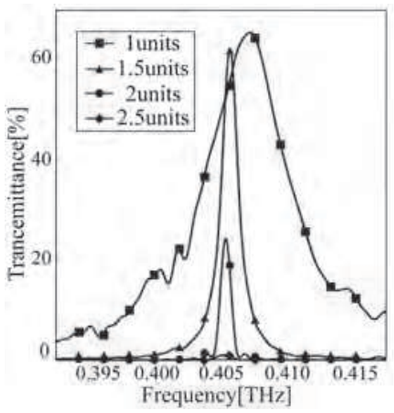

Fig. 9. Calculated peak profiles of multiple resonation modes in water cells of plane defects put between photonic crystals with various layer numbers.

5. Smart processing

5.1 Dielectric components

The photonic crystal resonators of the terahertz wave were fabricated by using computer aided design and manufacturing of smart processing. The diamond lattices were designed by using a computer graphic software (Toyota Caelum Co. Ltd., Japan, Think-Design Ver. 9.0). The lattice constant of the diamond structure and the aspect ratio of the dielectric lattice were 500 μm and 1.5, respectively. The whole size of the crystal component was 5×5×1 mm consisting of 10×10×2 unit cells. The designed model was converted into stereolithographic files of a rapid prototyping format and sliced into a series of two dimensional cross sectional data of 15 μm in layer thickness. These data were transferred into a micro stereolithographic equipment (D-MEC Co. Ltd., Japan, SI-C 1000). Figure 10 shows a schematic illustration of the micro stereolithography system. Photosensitive acrylic resins including alumina particles of 170 nm in average diameter at 40 % in volume content were supplied on a glass substrate from a dispenser nozzle by the air pressure. This paste was spread uniformly by using a mechanically controlled knife edge. The thickness of each layer was set at 15 μm.

Two dimensional solid patterns are obtained by a light induced photo polymerization. High resolution image has been achieved by using a digital micro mirror device. In this optical device, micro aluminium mirrors of 14 μm in edge length were assembled with 1024×768 in numbers. Each mirror can be tilted independently by piezoelectric actuating. Through the layer by layer stacking under the computer control, the acrylic resin component with the alumina particles dispersion was obtained. The composite precursor was dewaxed at 600 °C for 2 hs and sintered at 1500 °C for 2 hs in the air atmosphere. Subsequently, in order to obtain a plane defect between the two diamond structures, a micro glass cell was also fabricated by using the micro stereolithography.

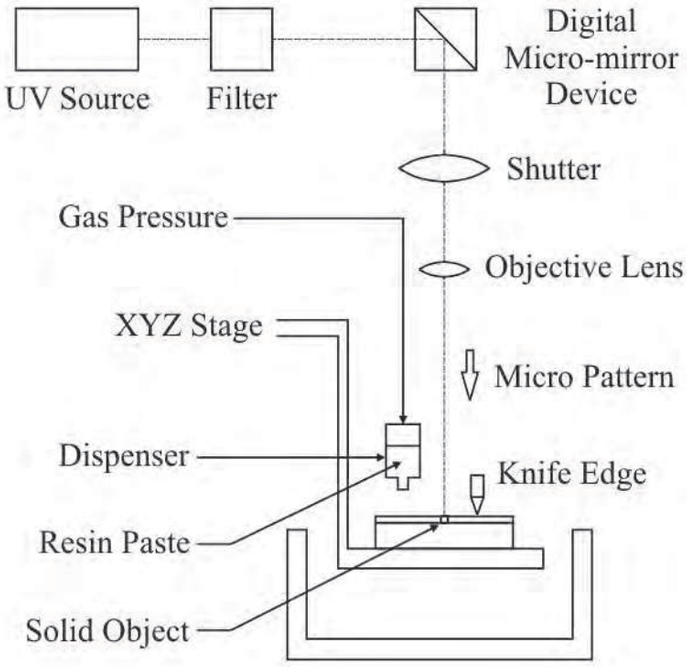

Fig. 10. A schematically illustrated free forming system of a micro stereolithography machine by using computer aided design and manufacturing (CAD/CAM) processes.

5.2 Device assembling

Figure 11-(a) shows the schematically illustrated components of the resonance cells. The quartz plates of 160 μm in thickness were inserted into the photosensitive acrylic resins in the stacking and exposing process. Finally, the micro resonators cell was put between the diamond photonic crystals, and the terahertz wave resonator was integrated successfully by using acrylic resin flames as shown in Figure 11-(b). These flames were glued together by using the photo sensitive liquid resin and the ultraviolet exposure solidification. Water solutions were infused through catheters connected on the top side of the resonance cell. The transmission properties of incident terahertz waves were analyzed by using the terahertz spectroscopy. The distributions of electric field intensities in the resonator were simulated and visualized at the localized frequency by using the transmission line modelling.

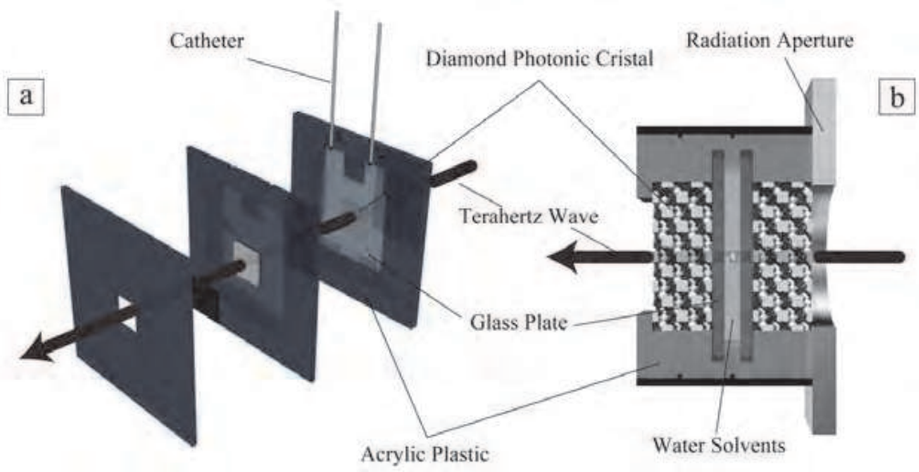

Fig. 11. A schematic illustration of the parts of the resonance cells (a), and fabricated THz wave resonator (b). The resonator was successfully created by integrating the diamond structures into the cells to realize multiple resonations of the THz wave in aqueous phase.

5.3 Spectroscopic evaluations

A terahertz wave attenuation of transmission amplitudes through the diamond photonic crystals were measured by using a terahertz time domain spectrometer (TDS) apparatus (Advanced Infrared Spectroscopy Co. Ltd., Japan, Pulse-IRS 1000). Figure 12 shows the schematic illustration of the measurement system. Femto second laser beams were irradiated into a micro emission antenna formed on a semiconductor substrate to generate the terahertz wave pulses. The terahertz waves were transmitted through the micro patterned samples perpendicularly. The dielectric constant of the bulk samples were measured through a phase shift counting. Diffraction and resonation behaviours in the dielectric pattern were calculated theoretically by using a transmission line modelling (TLM) simulator (Flomerics, UK, Microstripes Ver. 7.5) of a finite difference time domain (FDTD) method.

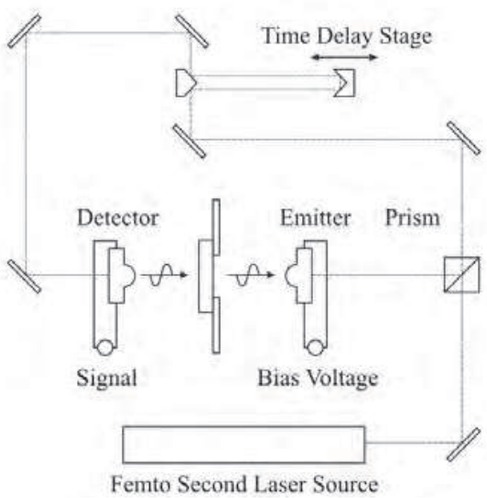

Fig. 12. The schematically illustrated measuring system of a terahertz wave analyzer by using a time domain spectroscopic (TDS) detect method.

6. Electromagnetic behaviours

6.1 Diamond structures

An alumina dispersed resin precursor fabricated by the micro stereolithography is shown in Fig. 13. The lattice constant of the formed diamond structure was 500 μm. The spatial resolution was approximately 0.5 %. The weight and color changes as a function of

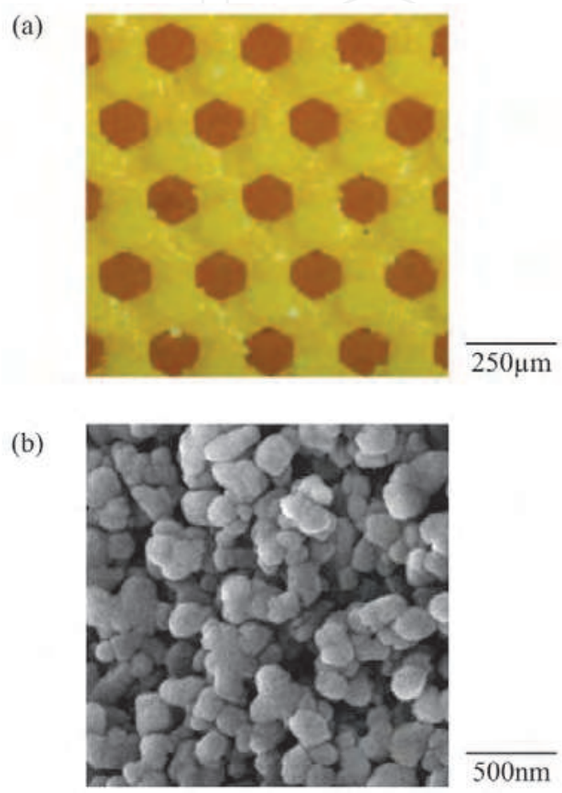

Fig. 13. The photonic crystal with the diamond structure composed of acrylic lattices with nano alumina particles dispersion formed by the micro stereolithography.

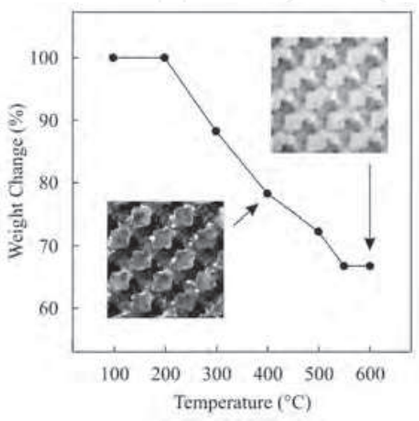

Fig. 14. The weight change as a function of temperature and the lattice color after dewaxing at 400 and 600°C in heating temperatures.

temperature are shown in Fig. 14. The sample color changed into black at 400°C due to carbonizing of resin. It became white at 600°C suggesting burning out of resin. Thus, the dewaxing process is considered to start at 200°C and complete at 600°C. The dewaxing temperature was optimized to be 600°C. Through the dewaxing and sintering processes, ceramic diamond structures were successfully obtained. Figure 15 shows (111), (100) and (110) planes of the sintered diamond structure composed of the micrometer order alumina lattice. The lattice constant was measured as 375 μm. The deformation and cracking were not observed. The linear shrinkage on the horizontal axis was 23.8 % and that on the vertical axis was 24.6 %. It is possible to obtain the uniform shrinkage by designing an appropriate elongated structure in the vertical direction for compensation to the gravity effect. The relative density reached 97.5 %. Dense alumina microstructure was formed, and the average grain size was approximately 2 μm. The measured dielectric constant of the lattice was about 10.

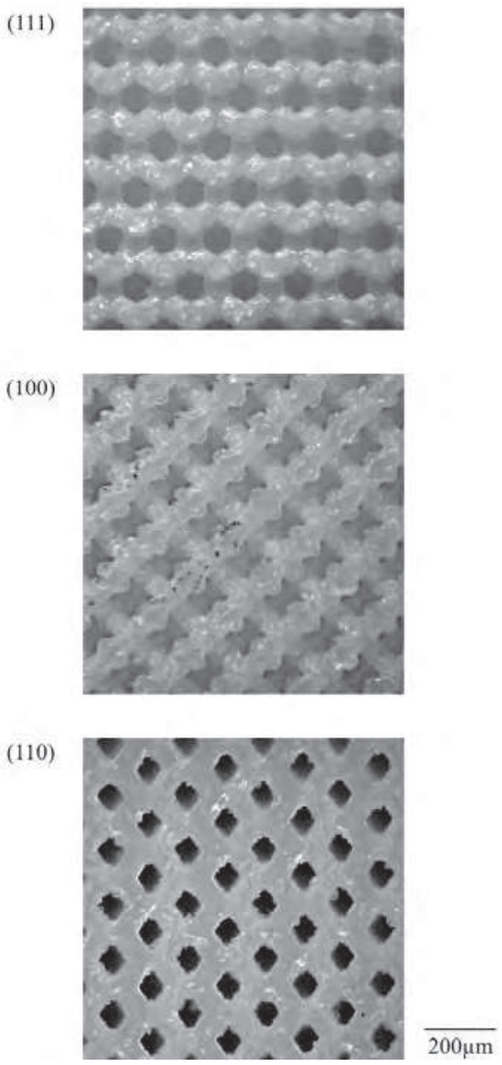

Fig. 15. Crystal planes of (111), (100) and (110) in alumina photonic crystals with the diamond structure fabricated by using the micro stereolithography. Sintering density of alumina lattices is 98.5 %. Dielectric constant of the lattice is 10.

6.2 Band structures

The terahertz wave attenuations of the transmission amplitudes through the alumina diamond structures for Γ-L <111>, Γ-X <100> and Γ-K <110> crystal directions are shown in Fig. 16. The forbidden gaps are formed at the frequency rages of 0.32 - 0.49, 0.35 - 0.53 and 0.35 - 0.52 THz in transmission spectra for Γ-L <111>, Γ-X <100> and Γ-K <110> directions, respectively. A common band gap was observed in every direction at the frequency range from 0.35 to 0.50 THz, where the electromagnetic wave cannot transmit through the crystal and is totally

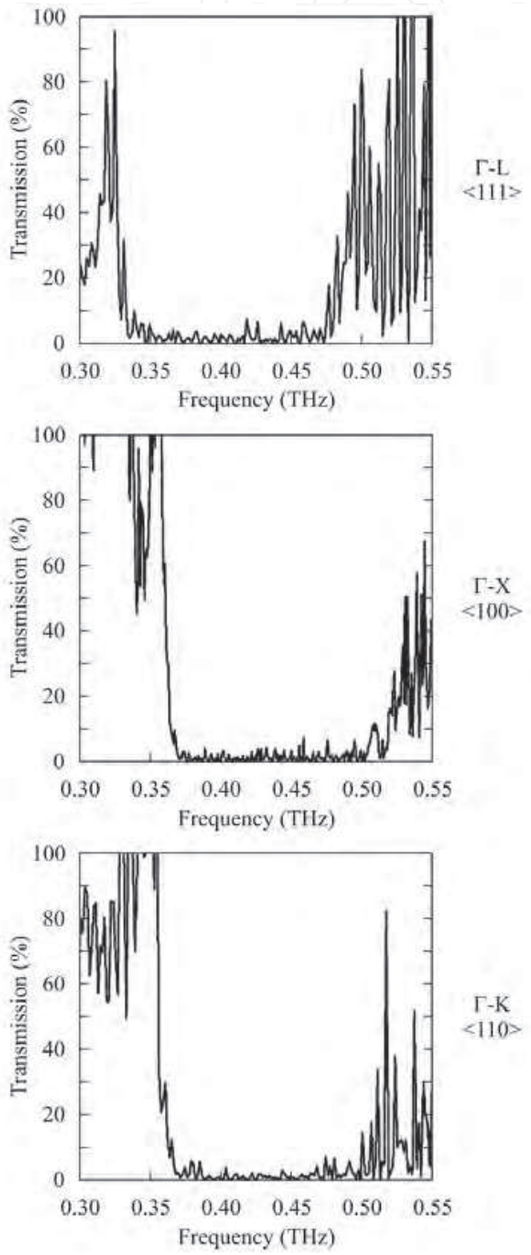

Fig. 16. Terahertz wave attenuations of transmission amplitude for Γ-L <111>, Γ-X <100> and Γ-K <110> directions in the alumina photonic crystal with the diamond structure by using terahertz time domain spectroscope.

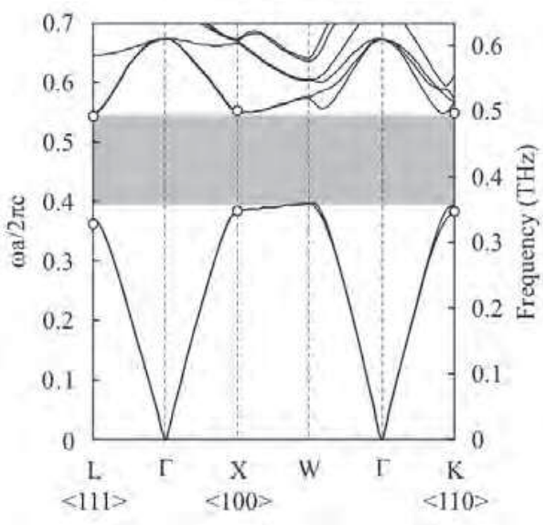

Fig. 17. A photonic band diagram calculated by plane wave expansion (PWE) method. Opened circles are measured edge frequencies of photonic band gaps. The dielectric constant of the lattice was 10. The frequency range with gray color indicates the perfect band gap in common for all directions.

reflected in all directions. The measured band gap frequencies were compared with calculation results by the plane wave expansion method as shown in Fig. 17. The band diagram of the photonic crystal along symmetry lines in the Brillouin zone is drawn theoretically by the PWE method. The opened circles mean the higher and lower edges of the measured band gaps. These frequency ranges of opaque regions corresponded to the calculation. According to the photonic band diagram, it was demonstrated that a complete photonic band gap opened between 0.35 and 0.49 THz. When a gap is formed, there are two types of the standing wave modes with the wavelength corresponding to periodicity of the dielectric lattices at the frequencies of the each band edges. The lower frequency mode concentrates the wave energy in the dielectric region, whereas the higher frequency mode concentrates in the air region.

6.3 Localized modes

The integrated terahertz wave resonator is shown in Fig. 18. The two diamond lattice components were attached on the quartz glasses, and these two glass plates were arranged with 150 μm in parallel interval. The tolerance for the transmission direction of the electromagnetic wave was converged within 5 μm. The cell capacity was 0.02 ml. Figure 19-(a) shows the measured transmission spectra for the resonators. Distilled water or ethanol was infused into the micro cells. In the case of distilled water, two localized modes of transmission peaks were observed at 0.410 and 0.491 THz in frequencies in the photonic band gap. In the case of ethanol, an amplification peak was observed at 0.430 THz. The measured band gap ranges and the localized mode frequencies have good agreement with the simulated results by the transmission line modelling as shown in Fig. 19-(b). In the transmission spectrum through the photonic crystal resonator including the water, the localized modes of the higher and lower peak frequencies are defined mode A and B, respectively. And, the localized mode peak in the transmission spectrum through the ethanol is defined mode C. The cross sectional profiles of the electric field intensity

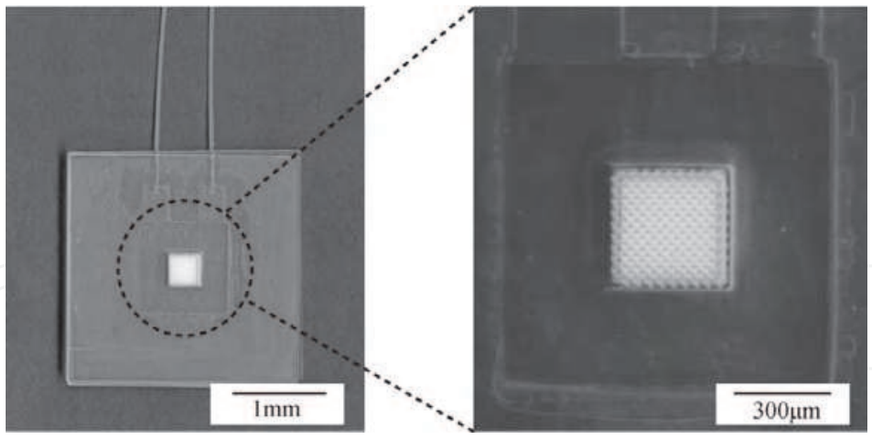

Fig. 18. A terahertz wave resonator with micro liquid cell sandwiched between diamond photonic crystals. Distilled water and ethanol were infused through the catheters implanting in the top side of the cells respectively.

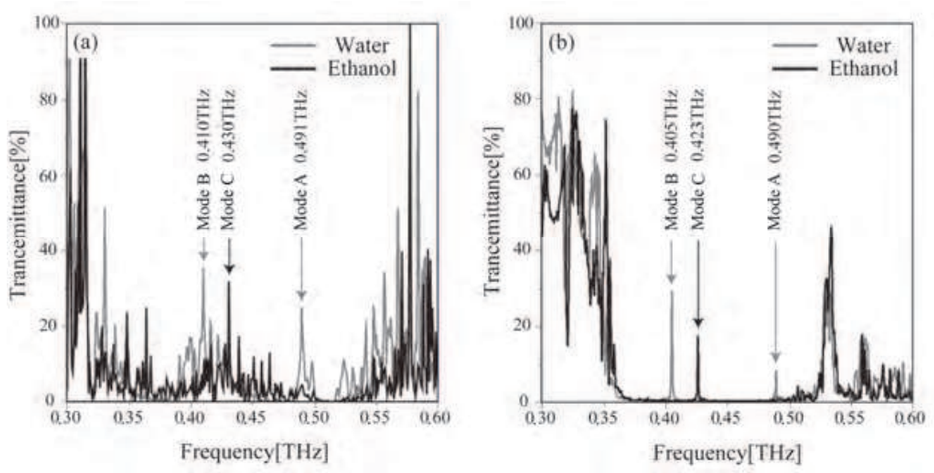

Fig. 19. Transmission spectra for the resonators infusing distilled water and ethanol. The spectra (a) and (b) are measured and calculated properties by using the terahertz wave time domain spectroscopy and a transmission line modeling methods, respectively.

corresponding to the localized mode A, B and C were simulated and visualized theoretically as shown in Fig. 20-(a), (b) and (c), respectively. The terahertz wave was propagated from the left to the right side. The white and black areas show that the electric field intensity is high and low, respectively. The incident terahertz waves were resonated and localized strongly through the multiple reflections in the liquid cell between two diffraction lattices with the diamond structures. Concerning with the localized mode A as shown in Fig. 20-(a), the standing wave with five nodes was observed in the vicinity area of the glass cell. And, the localized mode B with the lower frequency and the longer wavelength is composed of the standing wave with four nodes between the diffraction lattices as shown in Fig. 20-(b). Concerning with the localized mode C in the ethanol as shown in Fig. 20-(c), the standing wave with four nodes has the similar resonance profiles between the diffraction lattices as the localized mode B in the water. Figure 20-(d) shows the dielectric constants and

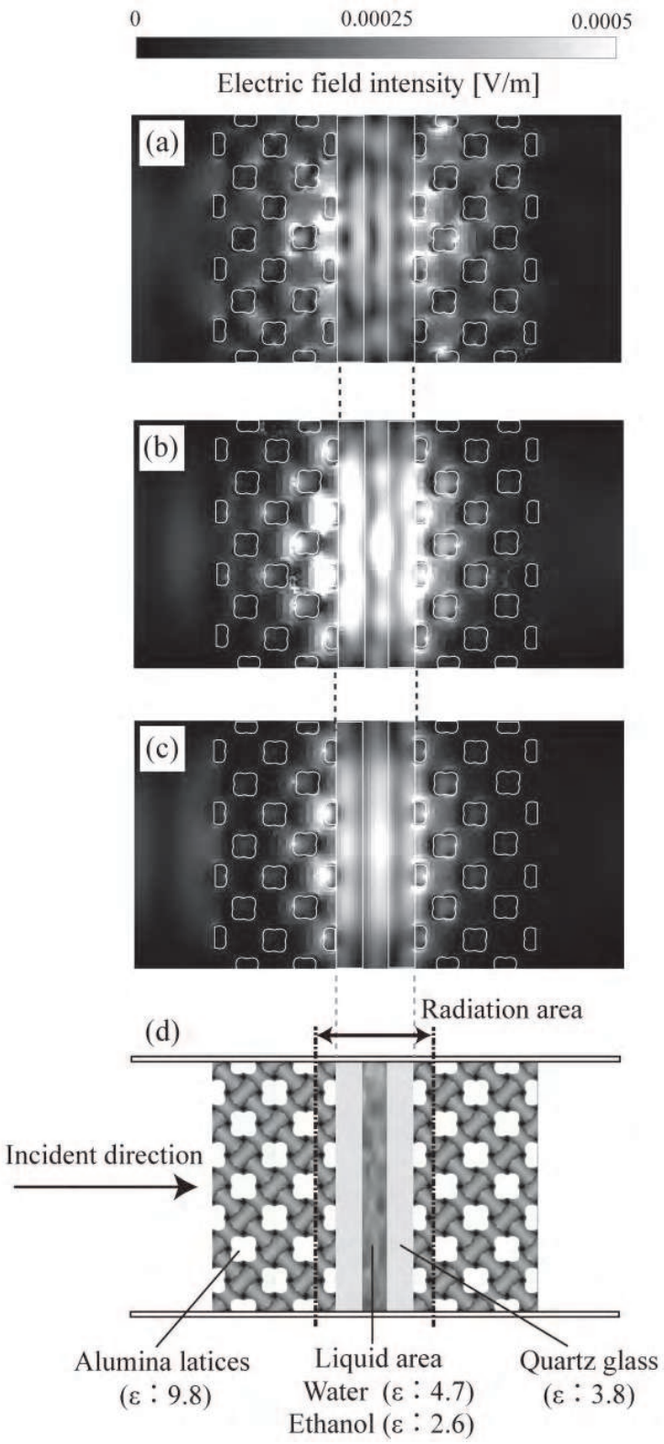

Fig. 20. Electric field distributions of localized modes simulated by transmission line modeling (TLM) method of a finite difference time domain (FDTD). The localized mode A, B and C, are shown in (a) , (b) and (c), respectively. Dielectric constants and composite dimensions of the photonic crystal resonator are shown in (d).

composite dimensions of the photonic crystal resonator. The dielectric constants of water and ethanol are 4.7 and 2.6 in the terahertz wave frequency range [17,18]. By using the terahertz wave time domain spectroscopy, the dielectric constants of alumina and quartz grass were measured as 9.8 and 3.8. In comparison with the resonance areas of the localized mode B and C, the effective dielectric constants decrease from 3.02 to 2.59, and the optical lengths decrease from 1.13 to 1.05 mm, respectively. Therefore, the resonance peak frequencies of the localized mode B and C with the similar standing wave profiles are shifted clearly from 0.410 to 0.430 THz by replacing the water with ethanol in the resonator. Form these results, the fabricated phonic crystal resonator is considered to be a promising candidate as the novel analytical device to determine the dissolved components in the aqueous solution by using the terahertz spectroscopy.

7. Conclusions

Terahertz wave resonators of a micro glass cell put between two photonic crystals composed of alumina lattices with a diamond structure were fabricated successfully by using micro stereolithography. Transmission spectra were measured through the photonic crystal resonators including pure water or ethanol. Localized modes of sharp transmission peaks were observed in the photonic band gaps. In a distribution profile of electric field intensity simulated by using transmission line modelling, the strong localized modes were formed through multiple reflections in the liquid regions between the diffraction lattices. Moreover, the localized mode peak was shifted clearly from higher to lower frequencies through replacing the pure water with the ethanol. The fabricated photonic crystal resonator is considered to be a promising candidate for novel analytical devices to detect the compositional variations in natural aqueous phase environments.

8. References

Akahane, Y., Asano, T., Song, B. & Noda, S. (2003). High-Q Photonic Nanocavity in a Two-Dimensional Photonic Crystal. Nature, Vol.425, (September 2003), pp.944-947.

Baba, T. & Fukuya, N. (2001). Light Propagation Characteristics of Defects Waveguides in a Photonic Crystal Slab. Photonic Crystals and Light Localization (edited M. Soukoulis), Kluwer Academic Publishers, Netherlands.

Chen, W,; Kirihara, S. & Miyamoto, Y. (2007a). Fabrication and Measurement of Micro Three-Dimensional Photonic Crystals of SiO_2 Ceramic for Terahertz Wave Applications. Joiurnal of the American Ceramic Society, Vol.90, No.7, (July, 2007), pp.2078-2081.

Chen, W.; Kirihara, S. & Miyamoto, Y. (2007b). Three-dimensional Microphotonic Crystals of ZrO2 Toughened Al2O3 for Terahertz wave applications. Applied Physics Letter, Vol.91, No.15, (October 2007b), pp.153507-1-3.

Chen, W.; Kirihara, S. & Miyamoto, Y. (2007c). Fabrication of Three-Dimensional Micro Photonic Crystals of Resin-Incorporating TiO_2 Particles and their Terahertz Wave Properties. Journal of the American Ceramic Society, Vol.90, No.1, (January 2007c), pp.92-96.

Chen, W.; Kirihara, S. & Miyamoto, Y. (2008). Static Tuning Band Gaps of Three-dimensional Photonic Crystals in Subterahertz Frequencies. Applied Physics Letters, Vol.92, (December 1990), pp.183504-1-3.

Clery, D. (2002). Brainstorming Their Way to an Imaging Revolution. Science, Vol.297, (August 2002), pp. 761- 763.

Cregan, R.; Mangan, B., Night, J., Birks, T., P. Russell, S., Roberts, P. & Allan, D. (1999). Singlemode Photonic Bandgap Guidance of Light in Air. Science, Vol.285, No.5433, (September 1999), pp.1537-1539.

Fischer B M, Walther M and Jepsen P Uhd 2002 Far-infrared vibrational modes of DNA components studied by terahertz time-domein spectroscopy Phys. Med. Biol. 47 3807-14.

Haus, J. (1994). A Brief Review of Theoretical Results for Photonic Band Structures. Journal of Modern Optics, Vol.41, No.2, (February 1994), pp.195-207.

Hineno, M. & Yoshinaga, H. (1974). Far-Infrared Spectra of Mono-, Di- and Tri-saccharides in 50-16

Ho, K.; Chan, C. and Soukoulis, C. (1990). Existence of a Photonic Gap in Periodic Dielectric Structures. Physical Review Letter, Vol.65, No.25, (December 1990), pp. 3152-3165.

John, S. (1987). Strong Localization of Photons in Certain Disordered Dielectric Superlattices. Physical Review Letter, Vol.58, No.23, (June 1987), pp.2486-2489.

Kanaoka, H.; Kirihara, S. and Miyamoto, Y. (2008). Terahertz Wave Properties of Alumina Microphotonic Crystals with a Diamond Structure. Journal of Materials Research, Vol.23, No.4, (April 2008), pp.1036-1041.

Kanehira, S.; Kirihara, S. & Miyamoto, Y. (2005). Fabrication of TiO_2-SiO_2 Photonic Crystals with Diamond Structure. Journal of the American Ceramic Society, Vol.88, No.6, (June 2005), pp.1461-1464.

Kawakami, S. (2000). Photonic Crystals, CMC, Tokyo.

Kawase K.; Ogawa, Y., Watanabe, Y. & Inoue, H. (2003). Non-destructive Terahertz Imaging of Illicit Drugs Using Spectral Fingerprints. Optics Express, Vol.11, Iss.20, (October 2003), pp.2549-2554.

Kirihara, S. & Miyamoto, Y. (2009) Terahertz Wave Control Using Ceramic Photonic Crystals with Diamond Structure Including Plane Defects Fabricated by Micro-stereolithography. The International Journal of Applied Ceramic Technology, Vol.6, No.1, (January, 2009), pp.41-44.

Kirihara, S.; Miyamoto, Y., Takenaga, K., Takeda, M. and Kajiyama, K. (2002). Fabrication of Electromagnetic Crystals with a Complete Diamond Structure by Stereolithography. Solid State Communications, Vol.121, No.8, (March, 2002), pp.435-439.

Kirihara, S.; Niki, T. & Kaneko, M. (2009a). Terahertz Wave Behaviors in Ceramic and Metal Structures Fabricated by Spatial Joining of Micro-stereolithography. Journal of Physics, Vol.165, No.1(April 2009), pp.12082-1-12082-6

Kirihara, S.; Niki, T. & Kaneko, M. (2009b). Three-dimensional Material Tectonics for Electromagnetic Wave Control by Using Micoro-stereolithography. Ferroelectrics, Vol. 387, (February 2009), pp.102-111.

Kirihara, S.; Takeda, M., Sakoda, K. and Miyamoto, Y. (2002a). Control of Microwave Emission from Electromagnetic Crystals by Lattice Modifications. Solid State Communications, Vol.124, No.4, (October 2002) pp.135-139,.

Kirihara, S.; Tsutsumi, K. & Miyamoto, Y. (2009c), Localization Behavior of Microwaves in Three-dimensional Menger Sponge Fractals Fabricated from Metallodielectric Cu/polyester Media. Science of Advanced Materials, Vol.1,No.2 (December 2009), pp.175-181.

Kosaka, H.; Kawashima, T., Tomita, A., Notomi, M., Tamamura, T., Sato, T. & Kawakami, S. (1999). Photonic Crystals for Micro Wave Circuits Using Wavelength-dependent Angular Beam Steering. Applied Physics Letter, Vol.74, No.8, (March 1999), pp. 1370-1378.

Kutteruf, M. R.; Brown, C. M., Iwaki, L. K., Campbell, M. B., Korter, T. M. & Heilweil, M. J. (2003). Terahertz Spectroscopy of Short-chain Polypeptides, Chem. Phys. Lett., Vol.375, (December 2003), pp.337-343.

Miyamoto, Y.; Kanaoka. H. & Kirihara, S. (2008). Terahertz Wave Localization at a Three-dimensional Ceramic Fractal Cavity in Photonic Crystals, Journal of Applied Physics, Vol.103, (May 2008), pp.103106-1-5.

Noda, S. (2000). Three-dimensional Photonic Crystals Operating at Optical Wavelength Region. Physica B, Vol.279, No.1-3, (April 2000), pp.142-149.

Noda, S.; Yamamoto, N., Kobayashi, H., Okano, M. and Tomoda, K., (1999). Optical Properties of Three-dimensional Photonic Crystals Based on III-V Semiconductors at Infrared to Near-infrared Wavelengths. Applied Physics Letters, Vol.75, No.16, (August 1999), pp.905-907,.

Ohtaka, K. (1979). Energy bang of photons and low energy photon diffraction. Physical Review B, Vol.19, No.10, (May 1979) pp.5057-5067.

Oyama, Y.; Zhen, L., Tanabe, T. & Kagaya, M. (2009). Sub-Terahertz Imaging of Defects in Building Blocks, NDT&E International, Vol.42, (January 2009), pp,28-33.

Oyama, Y.; Zhen. L., Tanabe, T. & Kagaya, M. (2008). Sub-Terahertz Imaging of Defects in Building Blocks. NDT&E International, Vol.42, No.1, (January 2008), pp.28-33.

Soukoulis, C. (1996). Photonic Band Gap Materials, Kluwer Academic Publsher, Netherlands.

Takano, H.; Song, B., Asano, T. & Noda, S. (2005). Highly Efficient in-Plane Channel Drop Filter in a Two-Dimensional Heterophotonic Crystal. Applied Physics Letters, Vol.86, No.24, (June, 2005), pp.241101-1-3.

Temelkuran, B.; Bayindir, M., Ozbay, E., Biswas, R., Sigalas, M., Tuttle, G. & Ho, K. (2000). Photonic Crystal-based Resonant Antenna with Very High Directivity. Journal of Applied Physics, Vol.87, No.1, (January 2000), pp.603-605.

Van Exter, M.; Fattinger, C. & Grischkowsky, D. (2002). Terahertz Time-domain Spectroscopy of Water Vapor. Optics Letters, Vol.14, Iss.20, (October 1989), pp.1128-1130.

Vos, W.; Sprik, R., Blaaderen, A., Imhof, A., Lagendijk, A. & Wegdam, G. (1996). Strong Effects of Photonic Band Structures on the Diffusion of Colloidal Crystals. Physical Review B, Vol.53, No.24, (February 1996), pp.16231-16235.

Wallace, V. P.; Fitzgerald, A. J., Shankar, S., Flanagan, N., et al. (2004). Terahertz Pulsed Imaging of Basal Cell Carcinoma ex Vivo and in Vivo. Br. J. Dermatol, Vol.151 (August 2004), pp.424–32.

Wallace, V.; Fitzgerald, A., Shankar, S. & Flanagan, N. (2004). Terahertz Pulsed Imaging of Basal Cell Carcinoma ex Vivo and in Vivo. The British Journal of Dermatology, Vol.151, No.2, (August, 2004), pp.424-432.

Woodward, R.; Wallace, V., Arnone, D., Linfield, E. & Pepper, M. (2003). Terahertz Pulsed Imaging of Skin Cancer in the Time and Frequency Domain. Journal of Biological Physics, Vol.29, No.2-3, (June 2003), pp.257-259.

Yablonovitch, E. (1987). Inhabited Spontaneous Emission in Solid-state Physics and Electronics. Physical Review Letter, Vol.58, No.20, (May 1987), pp. 2059-2062.

Yamaguchi, M.; Miyamaru, F., Yamamoto. K. › Tani, M. & Hangyo, M. (2005). Terahertz Absorption Apectra of L-, D-, and DL-alanine and Their Application to Determination of Enantiometric Composition. Appl. Phys. Lett, Vol. 86, (April 2005), pp.053903.

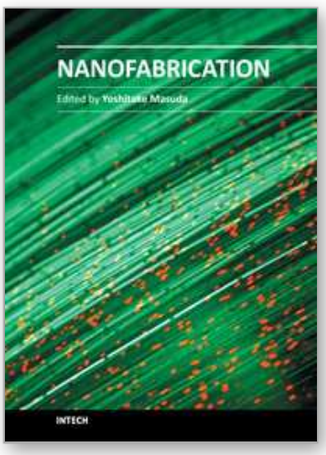

Nanofabrication

Edited by Dr. Yoshitake Masuda

ISBN 978-953-307-912-7
Hard cover, 354 pages
Publisher InTech
Published online 22, December, 2011
Published in print edition December, 2011

We face many challenges in the 21st century, such as sustainably meeting the world's growing demand for energy and consumer goods. I believe that new developments in science and technology will help solve many of these problems. Nanofabrication is one of the keys to the development of novel materials, devices and systems. Precise control of nanomaterials, nanostructures, nanodevices and their performances is essential for future innovations in technology. The book "Nanofabrication" provides the latest research developments in nanofabrication of organic and inorganic materials, biomaterials and hybrid materials. I hope that "Nanofabrication" will contribute to creating a brighter future for the next generation.

How to reference

In order to correctly reference this scholarly work, feel free to copy and paste the following:

Soshu Kirihara (2011). Fabrication of Photonic Crystal Cavities for Terahertz Wave Resonations, Nanofabrication, Dr. Yoshitake Masuda (Ed.), ISBN: 978-953-307-912-7, InTech, Available from: http://www.intechopen.com/books/nanofabrication/fabrication-of-photonic-crystal-cavities-for-terahertz-wave-resonations

INTECH
open science | open minds

InTech Europe
University Campus STeP Ri
Slavka Krautzeka 83/A
51000 Rijeka, Croatia
Phone: +385 (51) 770 447
Fax: +385 (51) 686 166
www.intechopen.com

InTech China
Unit 405, Office Block, Hotel Equatorial Shanghai
No.65, Yan An Road (West), Shanghai, 200040, China
中国上海市延安西路65号上海国际贵都大饭店办公楼405单元
Phone: +86-21-62489820
Fax: +86-21-62489821

IntechOpen